Chemical Engineering Science 281 (2023) 119083

Contents lists available at ScienceDirect

Chemical Engineering Science

journal homepage: www.elsevier.com/locate/ces

Effect of alcohols on CO_2 absorption, phase splitting, and desorption behaviors of biphasic anhydrous system: The primary amine-tertiary amine of DGA-PMDETA

Ziwei Shen [a], Siyang Tang [a,*], Houfang Lu [a,b], Shan Zhong [a], Lei Song [a], Hongjiao Li [a], Bin Liang [a,b]

[a] Laboratory of Low-Carbon Technology and Chemical Reaction Engineering, School of Chemical Engineering, Sichuan University, Chengdu 610065, China
[b] Institute of New Energy and Low-Carbon Technology, Sichuan University, Chengdu 610207, China

ARTICLE INFO

Keywords:
Biphasic absorbent
Anhydrous absorbent
Phase splitting
CO_2 capture
Alcohol

ABSTRACT

Chemical absorption with organic amine solution is the most mature technology for CO_2 capture. Some biphasic anhydrous absorbents show potential in reducing regeneration energy consumption, but high viscosity of the CO_2 rich phase hinders its practical application. Alcohols are commonly employed as dilutes to reduce viscosity reducers, while its effect on CO_2 absorption and phase splitting behaviors are still unclear. In this study, the effects of alcohols on CO_2 absorption and phase-splitting of biphasic anhydrous 2-(2-Aminoethoxy)ethanol (DGA) -N,N,N′,N″,N″-pentamethyl diethylenetriamine (PMDETA) -alcohol systems are investigates. Adding alcohol reduces the viscosity of the CO_2-rich phase, enhances desorption rate, and decreases the phase splitting time. The rich phase entrainment stage and the rich phase thickening stage, can be distinguished along with during CO_2 absorption. The majority DGA reacts with CO_2 in the rich phase since the phase splitting begins. This work may provide some basis for further biphasic absorbent design and regulation.

1. Introduction

Carbon capture, utilization, and storage (CCUS), as a carbon dioxide (CO_2) sequestration strategy to relieve greenhouse effects, has gained increasing interest in the industry since the 2010 s (Deng et al., 2022). Currently, CO_2 absorption is one of the principal techniques for carbon capture (Nawaz et al., 2022). Monoethanolamine (MEA) aqueous system, methyldiethanolamine (MDEA) aqueous system and Benfield solution commercialized for decades have become the benchmark to evaluate new CO_2 absorbents (Fang et al., 2020; Mores et al., 2011; Shakerian et al., 2015). High energy consumption, high solvent loss and strong corrosion of these traditional absorbents limit the large-scale application for CO_2 capture. Anhydrous phase splitting absorbent, one of the phase transfer absorbents, is homogeneous before CO_2 absorption but heterogeneous after CO_2 absorption (a CO_2 rich phase and a CO_2 lean phase) (Xu et al., 2019; Barnea and Mizrahi, 1975). It cuts off the energy consumption of CO_2 desorption process by minimizing the amount of desorption liquid and replacing water with the solvent of lower sensible heat (Papadopoulos et al., 2019). In practice, the presence of water in the CO_2 source may accumulate in the anhydrous absorbent during the CO_2 absorption. It impacts both the absorption performance and phase splitting behavior of anhydrous absorbents. Some reports shows that the water balance of the lean-water or anhydrous absorbents during CO_2 capture can still be achieved by controlling desorption conditions (Zhang et al., 2019) (Shen et al., 2023). These anhydrous absorbents are proposed for CO_2 capture from gas mixtures after dehydration, such as acid gas remove from natural gas after dehydration.

In the anhydrous phase-splitting system, a primary/secondary amine usually plays the key CO_2 absorbent role, while alcohol or tertiary amine is taken as the key phase separation agent. Various anhydrous phase-splitting systems are reported, including primary/secondary amine + alcohol system (such as ethanol/1-propanol - tetramethylammonium glycinate ([N1111][Gly]) (Jiang et al., 2021), MEA/diethanolamine (DEA) - long-chain alcohols(Kim et al., 2014), 2-(ethylamino) ethanol (EMEA)-diethylene glycol diethyl ether (DEGDEE) (Barzagli et al., 2017)) and primary/secondary amine + tertiary system (such as, triethylenetetramine (TETA)- N,N-dimethylcyclohexylamine (DMCA),

* Corresponding author.
E-mail address: siyangtang@scu.edu.cn (S. Tang).

https://doi.org/10.1016/j.ces.2023.119083
Received 18 February 2023; Received in revised form 27 June 2023; Accepted 10 July 2023
Available online 21 July 2023

TETA- N, N, N′, N″, N‴-pentamethyl diethylenetriamine (PMDETA) (Zhang et al., 2018), aminoethylethanolamine (AEEA)- dimethyl sulfoxide (DMSO)-PMDETA(Zhou et al., 2020)). The phase splitting mechanism (Jiang et al., 2020) and molecular design regulation (a phase-splitting diagram for amine + alcohol anhydrous systems) have been proposed (Zhao et al., 2021). The carbamate solubility of the amine-CO_2 product (carbamate) in tertiary amines has been experimentally proved vital to phase-splitting behavior during CO_2 absorption (Li et al., 2022). Due to the high viscosity of amine-CO_2 product (carbamate), the CO_2-rich phase with a poor mobility may limits its further application.

To adjust the viscosity of CO_2-rich phase, more components are designed into the system, such as sulfoxide, sulfone and short chain alcohols (Zhou et al., 2020). Alcohols are reported to work as diluents to minimize the viscosity of the CO_2 rich phase but not to react with CO_2. These are believed to improve the gas–liquid mass transfer, heat transfer, phase splitting behavior, and fluid transport (Sarmad et al., 2017). These researches focus on CO_2 absorption capacity and phase splitting ratio of the new poly-component systems. Meanwhile the effect of the third component (alcohol) on phase splitting behavior, including phase separation rate, composition of the upper and lower phase, is unclear. And those phase splitting characters is vital to determine the mass transfer in the absorption column and residence time in the phase separator. The indistinct phase splitting behaviors limits the further biphasic absorbent design and the absorption reactor.

In this work, the primary amine 2-(2-Aminoethoxy)ethanol (DGA) - tertiary amine PMDETA system is selected as the typical biphasic anhydrous system from our previous research to study the regulation and influence of alcohols (Li et al., 2022). DGA, as a primary amine, is reported with a high reaction enthalpy, high absorption rate and larger capacity for absorption compared to secondary and tertiary amines (Lia and Rochelle, 2014). And it is widely utilized for CO_2 and SO_2 absorption (Salkuyeh and Mofarahi, 2012). DGA anhydrous systems also show higher absorption rates and desorption rates comparing to the 5 M MEA in our preliminary study. Although MEA is more commonly used for CO_2 capture compared to DGA, the MEA-PMDETA anhydrous system, MEA-TMEEA anhydrous system and MEA-TMPDA anhydrous system are heterogeneous before and after CO_2 absorption at the mass ratio of primary/secondary amine to tertiary amine at 1:1. Therefore, DGA is selected as the primary amine in this study (Li et al., 2022). It forms a biphasic anhydrous system with the agent with multiple tertiary amine groups, such as PMDETA, N,N,N'N'Tetramethyl-1,3-propanediamine (TMPDA) and N,N,N',N'-Tetramethyl ethylenediamine (TMEEA). PMDETA, a powerful Brønsted base, may work as a phase separation agent with different primary/secondary amines, such as DEA, MEA, 3-Aminopropan-1-ol (3AP) and 4-Amino-1-Butanol (4AB). The viscosity of CO_2 rich phase of DGA-PMDETA is relatively high. Several short chain alcohols are selected as diluents and added into the system. The influence of alcohol on CO_2 absorption and desorption, phase splitting behavior, desorption energy consumption is investigated. The characteristics of phase splitting behavior during CO_2 absorption process has been recognized.

2. Experiments and calculations

2.1. Absorption, phase separation and desorption

MEA (GR,99 %), DGA (GR,98 %), PMDETA (AR,99 %), glycol ethylene (EG, AR,99 %), 1-butanol (NBA, AR,99 %), 1,4-butanediol (BDO, AR,99 %), 1,2-propanediol (PDO, AR,99 %), glycerol (Gl, AR, 99 %) were purchased from Adamas, Shanghai Titan and TCI. CO_2 (>99 %), N_2(>99.9 %) were purchased form Chengdu Dongfeng Gas Co., Ltd., China. All absorbents in this work are set with certain primary amine (DGA or MEA) and certain other solvents. 3MEA is short for 30 wt % MEA aqueous system, while 3D6P-1EG is short for the system with 30 wt % DGA, 60 wt % PMDETA and 10 wt % EG.

CO_2 Absorption is carried out in a 250 mL three-neck flask with magnetic stirring (Fig. 1). A thermostatic water bath (DF101S, Hangzhou jingfei Co., ±1 K) is used to control the temperature. The gas controlled by the gas mass flow meters r (MFC, Beijing Sevenstar Electronics Co., Ltd., China) is injected the three-neck flask. The exhaust gas sequentially passes through a condensing pipe, acid bottle, drying tube and a portable infrared CO_2 IR analyzer (YCC-PTM600-CO2, Shenzhen Yichuang technology Co., LTD, China, ± 0.2 %). The CO_2 concertation of the exhaust gas detected by the IR analyzer is automatically recorded. Before the reaction, N_2 is firstly injected at a flow rate of 420 mL/min to replace the air in the gas pipeline and the reactor. Then 50 g of absorbent is injected into the reactor. The magnetic stirring device is turn on with a rotation speed of 700 r/min. After 10 mins, the system would be stable at 313 K, and the CO_2 concentration shown in infrared CO_2 IR analyzer would be 0 %. To start the reaction, 60 mL/min CO_2 is injected into the reactor together with the N_2. Here, the total gas flow rate is 480 mL/min, and the gas mixture contains 12.5 % CO_2 and 87.5 % N_2. When the CO_2 concentration shown in the IR analyzer reaches 12.5 % (±0.2 %), it states that no more CO_2 is absorbed in the reactor. Then the reaction is terminated.

After absorption, the absorbent automatically splits into two phases, CO_2-lean phase on the top and CO_2-rich phase on the bottom. The CO_2-rich phase is collected for further desorption. The desorption device is same with the absorption device. It is firstly purged with N_2 at a flow rate of 200 mL/min. Desorption temperature is set at the desired temperature (363–393 K). Then 10 g of CO_2-rich liquid would be injected into it. The magnetic stirring is turn on. CO_2 desorbed form the system is carried by N_2 into the IR analyzer. When the CO_2 concentration shown in IR analyzer is less than 0.5 %, desorption would be terminated. The CO_2 loading of the solvent is determined using the hydrochloric acid titration (supporting information). The titration error is about 1 mL CO_2 gas.

N_2 is inert in CO_2 absorption and desorption. The absorption rate (r_{abs}) and desorption rate (r_{des}) are calculated as Eq.1–2.

$$r_{abs} = [Q_0 - Q_1]/m_{abs} \tag{1}$$

$$r_{des} = [Q_{N_2}/(1-y) - Q_{N_2}]/m_{des} \tag{2}$$

where m is solution quality (g), Q_0 is CO_2 molar flow rate before absorption, Q_1 is CO_2 molar flow rate after absorption, Q_{N2} is N_2 molar flow rate.

In this work, the phase splitting time is defined as the minimum time required for liquid–liquid phase separation from the highly mixed two phases to produce two distinct horizontal interfaces (Kaul et al., 1995). A cylindrical glass flask with a diameter of 65 mm and a height of 70 mm is used to measure the phase splitting time. The flask is sink in a thermostatic water bath with a magnetic stirring. CO_2 absorption is basically same with the former absorption steps. But the CO_2 absorption would be terminated at different time. The magnetic stirring is stopped at the moment of CO_2 absorption termination. The phase splitting time would be recorded from the moment of the string stop to the moment of the emergence of a clear two-phase interface unchanged.

Gas chromatography (GC, column: KB-624 (30 m × 0.53 mm × 3.00 μm)) is used to quantify the mass variations of various compounds in the upper and lower phases. Nuclear magnetic resonance (NMR, Bruker AV-II-400 MHz NMR spectrometer) is used to identify materials of the solvent before and after desorption. The simultaneous thermal analysis (STA 449F3 Jupiter, Netsch, Germany) is employed to test the mass change and heat flow changes during the absorption. Differential scanning calorimetry (DSC, Netzsch DSC 214) is used to test the heat capacity at constant pressure. Viscosity is tested by the rotating viscometer (LV-DV2T, Shanghai Fangrui, China). Density is tested with a 5 mL specific gravity flask (Supporting Information).

All the experiments are performed in triplicate. And the results used in this study is average results of three replicated results.

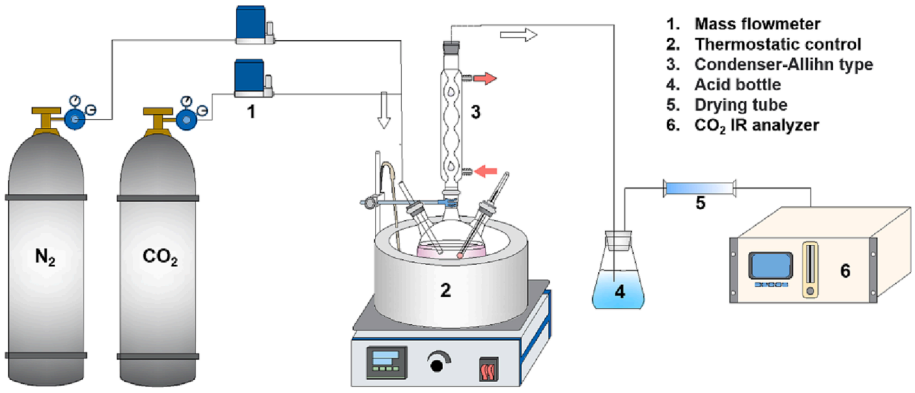

Fig. 1. CO_2 absorption experimental device.

2.2. Energy consumption calculation

In the traditional absorption technology, the CO_2 rich phase liquid is heated to a required temperature, then delivered to the desorption tower. Subsequently, the CO_2-lean liquid after desorption would be resent to the absorption tower. The desorption energy includes reaction enthalpy (Q_{reac}), sensible heat of desorption liquid (Q_{sen}), and latent heat of vaporization (Q_{evap}) (Nwaoha et al., 2017). The following regeneration conditions are assumed to appropriately evaluate the energy consumption of thermal regeneration as follows (Zhu et al., 2020):

1. The absorbent absorb CO_2 completely to reach the equilibrium in the absorption tower, and all CO_2-rich phase liquid is transported into the desorption tower after phase splitting;
2. The absorption is performed at 313 K, and the CO_2-rich phase solution is heated to 353 K through a heat exchanger. The desorption temperature of the biphasic absorbents is 373 K;
3. The regeneration ratio of the biphasic absorbents is set as 89 % according to the following experimental data ;
4. Since the boiling temperatures of DGA, PMDETA, EG, BDO, PDO, Gl, and NBA are much greater than the desorption temperature (Table S2), the Q_{evap} is disregarded in the calculation;
5. Theoretically, the correlation constant (m-n) of the heat exchangers varies with solvent viscosity, and is typically between 0.1 and 0.5 (Zhao et al., 2018). Due to the high viscosity of the rich phase, and the correction coefficient is assumed as 0.5;
6. The viscosity of CO_2-rich phase- tested at 353 K are used for calculation.

The sensible heat of two-phase absorbent is modified with the correction factor χ, which is linked to the phase splitting ratio, physical characters, and heat exchanger parameters (dimensionless correlation) (Liu et al., 2019b). Since the average temperature of the heat exchangers between CO_2-rich phase and desorbed CO_2-rich liquid is 353 K (Nwaoha et al., 2017), the viscosity of CO_2-rich phase at 353 K is used for sensible heat adjustment. Considering the reboiler load, optimization of operating parameters and heat recovery, 50 % of Q_{sen} is assumed recovered (Li et al., 2013). The desorption energy consumption is calculated as follows (Eq.3–7):

$$Q^{*}_{reg} = Q_{reac} + \chi Q_{sen} + Q_{evap} \tag{3}$$

$$Q_{reac} = \frac{\Delta H}{M_{rco_2}} \tag{4}$$

$$Q_{sen} = \frac{C_P \cdot \Delta T}{C_{co_2} \theta M_{rco_2}} \tag{5}$$

$$Q_{evap} = \frac{n_w \times \Delta H_{H_2O}}{n_{co_2} \times M_{co_2}} \tag{6}$$

$$\chi = \psi \frac{C_P}{C_P^{MEA}} \left(\frac{\mu}{\mu_{MEA}}\right)^{m-n} \tag{7}$$

$Mrco_2$ is CO_2 molecular mass (44 g/mol), ΔT is the temperature difference between the top and bottom of the desorption tower, θ is the absorbent regeneration rate, ψ is volume ratio of the rich phase, μ is viscosity at 353 K, ΔH is reaction enthalpy (kJ/mol), C_P is specific heat capacity at constant pressure ($kJ \cdot kg^{-1} \cdot K^{-1}$); m-n is the correlation constant of the heat exchangers. More details are available in Supporting Information.

3. Results and discussion

3.1. Alcohol effect on CO_2 absorption capacity of DGA-PMDETA

All the absorbents (except 3MEA) before CO_2 absorption are light yellow and homogeneous. After absorption, the upper phase (PMDETA phase, CO_2-lean phase) is clear and has good fluidity. The lower phase (CO_2-rich phase, CO_2 absorption product) is light yellow and viscous. CO_2 absorption performances of DGA-PMDETA alcohol systems were investigated (Fig. 2).

Phase splitting is observed during CO_2 absorption with anhydrous DGA-PMDETA systems at the weight ratio of DGA/PMDETA between 2:8 and 8:2. The polarity difference between DGA and DGA-CO_2 carbamates drives the phase splitting in this system (Li et al., 2022). When CO_2 absorption saturated, the volume ratios of upper and lower phase are related to the CO_2 absorption equilibrium (Zhan et al., 2020). PMDETA acts as the physical phase separation agent, which barely affects the reaction equilibrium. Therefore, the rich phase volume ratio varies linearly with the DGA fraction of the absorbent as shown in Fig. 2 (a). The CO_2 loading of the solvent almost varies linearly with the DGA fraction of the absorbent (Fig. 2(b)).

Over 97 % CO_2 exists in the rich phase after absorption (Fig. 2(b)). The CO_2 loadings of the upper phases are 0.26–0.33 mol CO_2/kg upper phase, which is basically the same as our previous report of 2.67 g carbamate /100 g tertiary amine (Li et al., 2022). It indicates that the carbamate from DGA and CO_2 partially physically dissolves in PMDETA. The CO_2 loading of the rich phase of 2D8P and 3D7P are slightly greater than those in other systems. Similar phenomenon of a higher CO_2 loading of the rich phase at a lower primary amine/tertiary amine ratio has also been reported (Pinto et al., 2014). At a lower DGA/PMDETA ratio, more DGA dissolves into the upper phase. It leads to a lower volume ratio of the lower phase (Fig. 2(a)) and a higher CO_2 loading of the lower phase (Zhou et al., 2017).

As discussed above, the rich phase volume ratio (y) linearly varies with the DGA fraction of the absorbent (x) as Eq. (8), while CO_2 loading

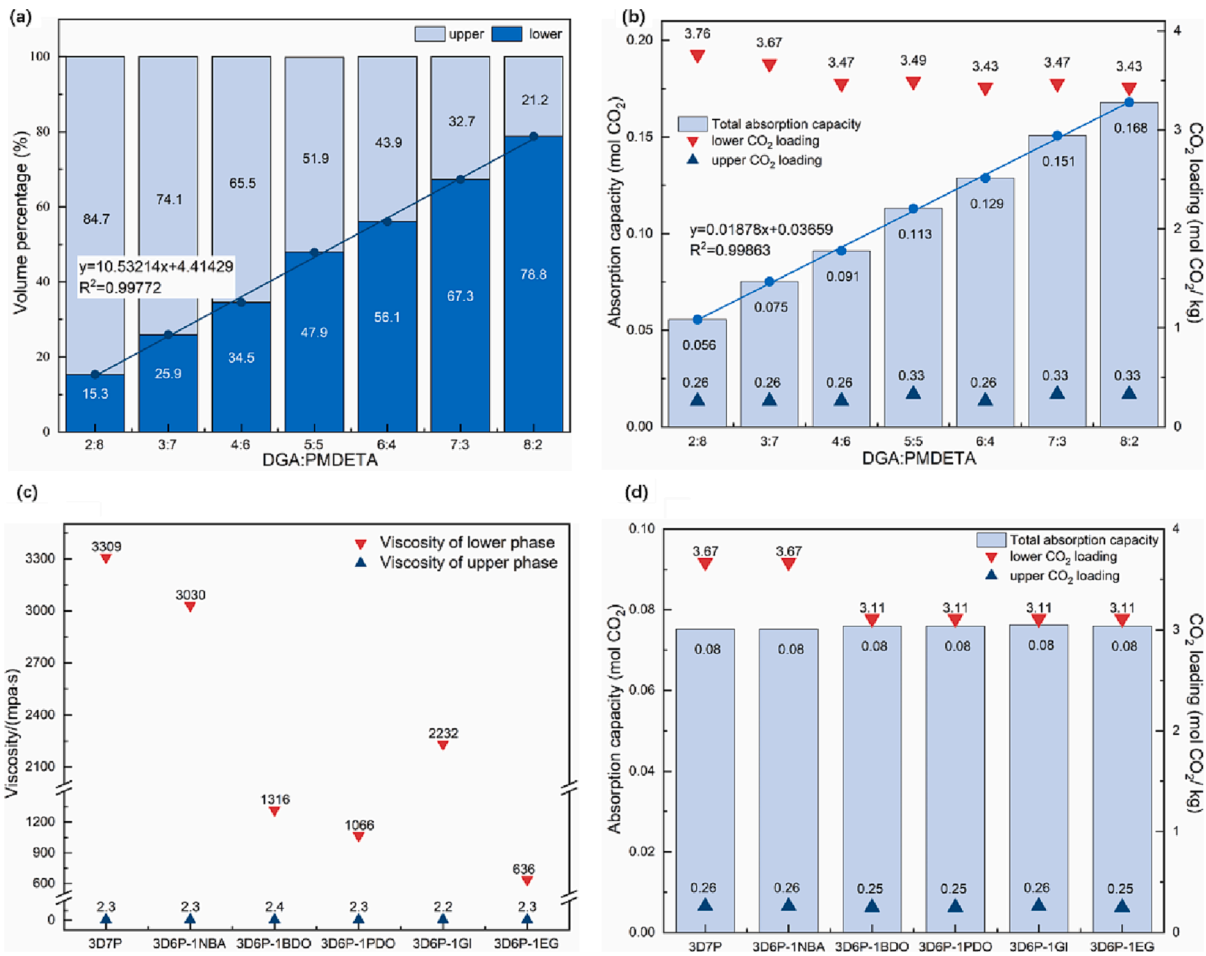

Fig. 2. CO_2 absorption of DGA-PMDETA systems, (a) phase splitting ratio of DGA-PMDETA systems with different DGA/PMDETA ratios at 313 K, (b) CO_2 loading of DGA-PMDETA systems with different DGA/PMDETA ratios at 313 K, (c) the viscosity of DGA-PMDETA systems (d) CO_2 loading of 3D6P-1alcohol at 313 K.

of the solvent (Y) linearly varies with the DGA fraction of the absorbent (x) as Eq. (9). It states the utilization ratio of primary amine are almost same among the DGA-PMDETA anhydrous systems. Despite the higher viscosity of the rich phase of the 3D7P system comparing to 2D8P, 30 wt. % DGA is selected for further research to comparing with the traditional amine system 30 wt % MEA aqueous system. Since the concentration of primary amine commonly used in industry is about 30 wt %, a mass ratio of DGA-PMDETA-alcohol systems are set as 30 % of DGA, 60 % of PMDETA, and 10 % of alcohols.

$$y = 10.53214x + 4.41429 \tag{8}$$

$$y = 0.01878x + 0.03659 \tag{9}$$

All alcohols (except NBA) act as diluents to minimize the viscosity of the CO_2 rich phase (Fig. 2(c)), while they barely affects absorption capacity (Fig. 2(d)). The viscosity of 3D7P is the highest, at 3309 mpa•s. The viscosity of the CO_2-rich phase of the 3D6P-1alcholes states as 3D6P-1Gl > 3D6P-1BDO > 3D6-1PDO > 3D6P-1EG, these is basically same with the viscosities of alcohols (Table S2). The viscosity of 3D6P-1Gl is still over 2000 mpa•s. Similar to other reports, NBA transfers into the CO_2 lean phase after CO_2 absorption (Zhao et al., 2022). NBA has a low density, and it is miscible with tertiary amines and enters in the upper phase. Therefore, the viscosity of the lower phase of 3D7P-1NBA barely changes comparing to that of 3D7P.

The addition of alcohols changes the volume ratio of upper phase or lower phase little. The volume ratio of CO_2 rich phase of 3D6P-1NBA is 25 %, which is basically the same as 3D7P of 25.9 %. The volume ratios of the rich phase of others systems are about 36.5 %, basically same with 4D6P of 34.5 %. The total CO_2 loading of 3D7P and 3D6P-1alcohols remains constant (Fig. 2(d)). The CO_2 loading in the lower phase of 3D7P-1NBA remains same with 3D7P systems, while the CO_2 loadings of the lower phase in other 3D6P-1alcohol systems decreases from 3.67 mol CO_2/kg to 3.11 mol CO_2/kg. The alcohol adding did not affect the absorption capacity. And it states that the decrease of CO_2 loading in the lower phase is caused by the transfer of alcohol. About 5.4 wt % more solvent transfers into the lower phase.

The circulation-regeneration experiments of 3D6P-1EG in Fig. S5 indicate that the biphasic absorbent solution is stable. The ^{13}CNMR spectra in Fig. S6 shows that PMDETA and EG do not participate into the CO_2 absorption reaction, and 3D6P-1EG may desorb completely (Kortunov et al., 2015; Kortunov et al., 2016). The regeneration rate of biphasic absorbents of DGA-PMDETA after CO_2 desorption could reach 89 %.

3.2. *Alcohol effect on CO_2 absorption and desorption rate*

The addition of alcohols affects CO_2 absorption (Fig. 3(a)) littler comparing to the DGA concentration of the absorbent (Fig. S7). The phase splitting happens at the first 5 mins during the CO_2 absorption. In the first 5 mins, the absorption rates of 3D7P and 3D6P-1alcohols are basically same. But after the phase splitting beginning, the absorption rates become different. The absorption rates of 3D6P-1alcohol are higher than 3D7P (purple line in Fig. 3(a)) after 25 mins CO_2 absorption. The 3D6P-1EG with a low viscosity of CO_2 rich phase has a higher absorption rate after phase splitting. Lower viscosity may improve the CO_2 absorption rate in a biphasic system by increasing the mass transfer.

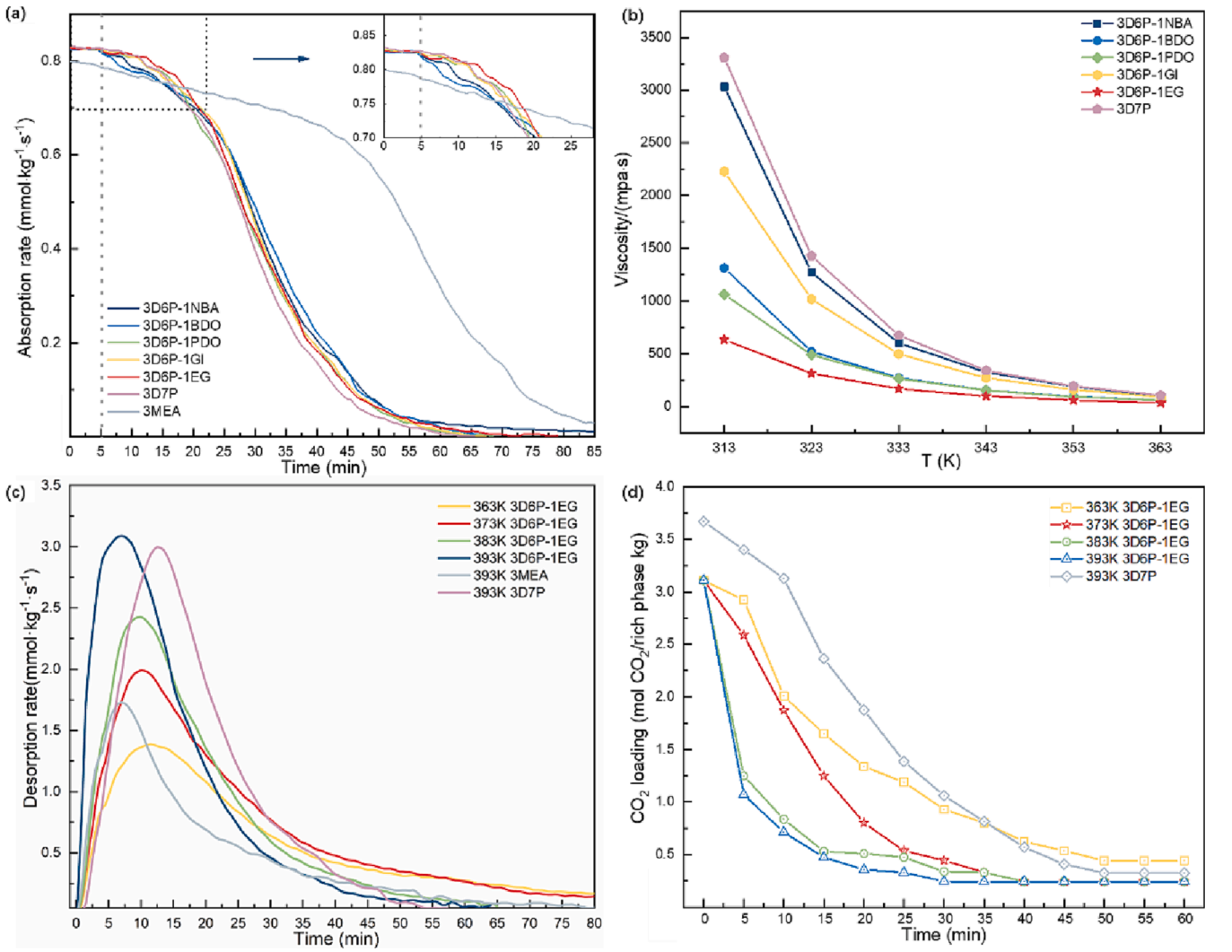

Fig. 3. CO_2 absorption and desorption performance (a) CO_2 absorption of 3D6P-1alcohol at 313 K, (b) viscosities of CO_2 rich phase at different temperature, (c) desorption rate of 3D6P-1EG at different temperatures, (b) CO_2-loading of lower phase during CO_2 desorption.

The desorption rate is believed to be significant for absorbent performance evaluation (Jin et al., 2022). The desorption behaviors of 3D6P-1EG, 3D7P and 3MEA are shown in Fig. 3(c-d). The alcohol EG benefits CO_2 desorption rate in the anhydrous systems. The highest desorption rate of 3D7P at 393 K and 3D6P-1EG at 373–393 K is greater than the desorption rate of 30 wt % MEA at 393 K. This is attributable to the fact that DGA with hydroxyl and ether linkages shows a negative effect on carbamate stability (Li et al., 2012).

Comparing the CO_2 desorption rates of 3D7P and 3D6P-1EG, the peak desorption rate of 3D7P is obviously delayed (Fig. 3(c)). In the rich phase for desorption, the DGA-CO_2 carbamate concentration of 3D7P (3.67 mol mol CO_2/kg) is higher than that of 3D6P-1EG (3.11 mol CO_2/kg). The original desorption rate of a higher concentration system should be theoretically higher at first. The viscosities of rich phases of 3D7P and 3D6P-1EG at 363 K are 108 mpa•s and 36 mpa•s. A low viscosity may improve gas–liquid mass transfer, heat transfer and fluid transport (Sarmad et al., 2017). Therefore, the delay in the peak desorption rate of 3D7P should be attributed to higher viscosity.

Generally, the desorption rate increases with the desorption temperature. CO_2 desorption of the rich phase of 3D6P-1EG at 393 K terminates at about 30 min, that of 3D6P-1EG at 373 K and 383 K terminates at 40 min, and those of 3D7P at 393 K and 3D6P-1EG at 363 K terminate at about 50 min. Although the desorption rate at 3D7P-1EG at 373 K is relatively slow, it could regenerate 90 % of CO_2 after 30 min of desorption. The CO_2 loading of 3D6P-1EG (373 K, 383 K, 393 K) after 50 min is almost same.

3.3. *Alcohol effect on phase splitting behavior during CO_2 absorption*

As discussed above, adding alcohols (except NBA) into DGA-PMDETA systems would lower the viscosity of the CO_2 rich phase and improve the CO_2 desorption rate. It also may regulate the phase splitting behavior. The phase splitting of two immiscible liquid phases in a stationary vessel is a kind of molecular diffusion. The phase splitting time is determined by molecular forces, gravity, and viscous forces (Boggione Santos et al., 2012). To investigate the effect of adding alcohols on the phase splitting, the phase splitting behaviors of 3D6P-1acohols during CO_2 absorption are examined every 5 min (Fig. 4).

The phase splitting happened at the first 5 min, with a CO_2 loading of the lower phase of 0.07 mol CO_2/mol amine (Fig. 4(a)). And the initial volume ratio of the lower phase of 3D6P-1alcohols is over 12 %, while it differs with the alcohols. The volume ratio of the lower phase increases gradually with CO_2 absorption until it reaches the CO_2 absorption equilibrium. The rich phase volume of 3D6P-1alcohols except 3D6P-1BDO tends to remain constant at 36.5 % after the CO_2 loading of 0.413 mol CO_2/mol amine. The dispersion zone caused by the higher viscosity can be observed at a higher CO_2 loadings over 0.476 mol CO_2/mol amine (Lin et al., 2015).

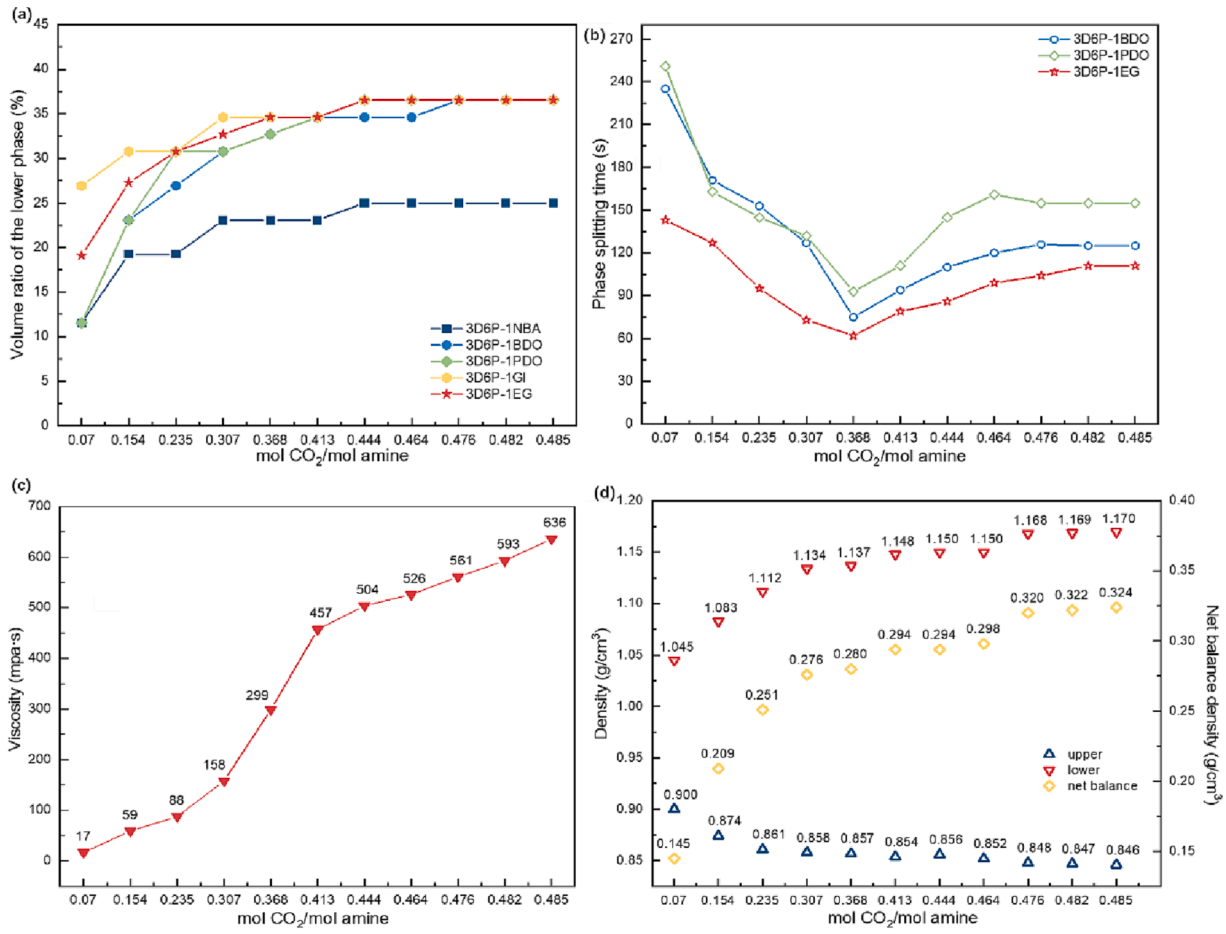

Fig. 4. Phase splitting behaviors of 3D6P-1acohol during CO_2 absorption, (a) volume ratio of the lower phase, (b) phase splitting time, (c) viscosity of CO_2 lower phase of 3D6P-1EG, (c) density of 3D6P-1EG.

Due to the high viscosity of rich phase of 3D6P-1GI and 3D6P-1NBA, detailed phase separation times of these two systems are not tested in this work (Fig. 4(b)). The phase splitting times are as follows 3D6P-1PDO > 3D6P1-BDO > 3D6P-1EG. The phase splitting time seems reliant on the density difference. The density of the alcohols are as follows: BDO of 1.016 g/cm^3, PDO of 1.036 g/cm^3, EG of 1.114 g/cm^3 (Mlllard, 2020). The density of the CO_2-rich phase are as follows: 3D6P-1PDO of 1.140 g/cm^3, 3D6P-1BDO of 1.146 g/cm^3, 3D6P-1EG of 1.169 g/cm^3. The CO_2-lean phase densities of the three absorbents (PMDETA phase) are the same of 0.857 g/cm^3. Gravity is the driving force for phase splitting. A greater density difference between the upper and lower phases may results in a shorter phase splitting time.

Remarkable turnings of the phase splitting time along with CO_2 loading could be observed. All the turning point of the curves are at the CO_2 loading of 0.368 mol CO_2/mol amine. Prior to this turning point, the phase splitting time decreases dramatically as CO_2 loading increaes. After this turning, the phase splitting time rises gradually. To clear this phenomenon, 3D6P-1EG system is taken as an example for further research (Liu et al., 2019a; Wang et al., 2022). The viscosity and density of 3D6P-1EG under CO_2 loading are tested (Fig. 4(c-d)). The 3D6P-1EG viscosity increases with the CO_2 loading increasing. The density of the upper phase of 3D6P-1EG decreases with the CO_2 loading increasing, while the density of the lower phase of 3D6P-1EG increasing with the CO_2 loading increasing (Fig. 4(d)). The increasing viscosity of the lower phase in the first stage (0.07–0.368 mol CO_2/mol amine) leads to an increase in the phase splitting time.However, the increase in the density difference of the upper and lower phases enhances the driving force (gravity), resulting in a decrease of the phase splitting time. In the first stage, the density difference of the upper and lower phase (gravity) dominates. In the second stage (0.368–0.485 mol CO_2/mol amine), the density difference of upper and lower phase increases slowly with CO_2 loading, and it has less impact on the splitting time.

To clear the basic factors affecting macroscopic viscosity, density and the phase splitting time, details composition of upper and lower phases of 3D6P-1EG with different CO_2 loading are characterized with GC

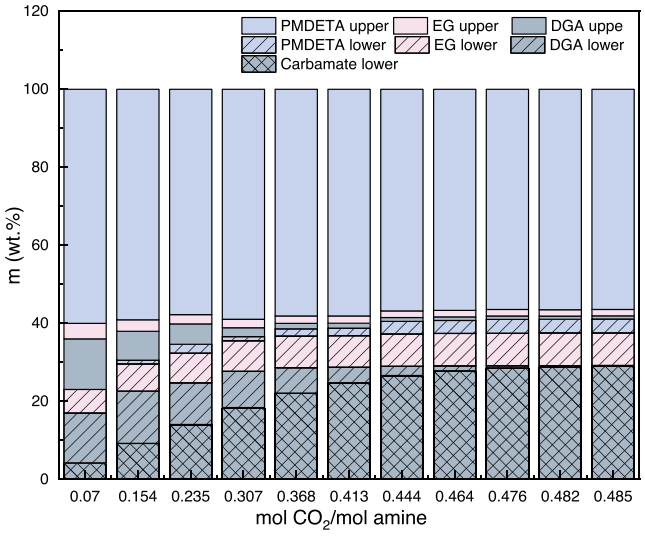

Fig. 5. The chemical components of the upper and lower phase of 3D7P-1EG during CO_2 absorption.

(Fig. 5). A total of 60.5 % EG dissolves in the lower phase at the beginning of phase splitting as a diluent. After the CO_2 loading of 0.482 mol CO_2/mol amine, 83.7 % of EG transfers into the lower phase, whereas 16.3 % EG remains in PMDETA phase. About 94.1 % PMDETA stays in the upper phase as a phase separation agent, while 5.9 % PMDETA presents as a strong Brønsted basic amine to form [PMDETA-H^+] and transfer into the lower phase (Kortunov et al., 2015). DGA works as both the diluent and the absorbent during CO_2 absorption. At the beginning of the phase splitting, only 14 % DGA reacts with CO_2 to form carbamate, while approximately 42.7 % of unreacted DGA transfers into the lower phase through the entrainment of carbamate. Some interaction between DGA, EG and DGA-CO_2 carbamate may occur in this stage. As the CO_2 loading increases, more carbamate forms, but the unreacted DGA gradually transfers into the lower phase. At the CO_2 loading of 0.368 mol CO_2/mol amine, 73.6 % DGA is in DGA-CO_2 carbamate, 21.9 % of unreacted DGA and 81 % EG is in the lower phase, only 4.5 % DGA and 19 % EG remains in the upper phase. At the CO_2 loading of 0.485 mol CO_2/mol amine, 2.6 % DGA is in the upper phase. After the CO_2 loading of 0.368 mol CO_2/mol amine, the DGA –CO_2 reaction mostly occurs in the lower phase.

As discussed above, the two phase splitting stages of anhydrous biphasic absorbent could be recognized as the rich phase entrainment stage and the rich phase thickening stage (Fig. 6).

The dispersion zone emerges concomitantly with the phase splitting. In the rich phase entrainment process (0–0.368 mol CO_2/mol amine of DGA-PMDETA-EG system), the lower phase volume increases, where CO_2-rich product cooperates with the most unreacted DGA and the most alcohols to transfer into the lower phase. The viscosity increases dramatically due to interactions between the DGA-CO_2 carbamate, DGA and EG, while the density difference between the lower phase gradually increases. Gravity dominates and the phase splitting time decreases gradually in this stage. In the rich phase-rich thickening stage (0.368–0.485 mol CO_2/mol amine of DGA-PMDETA system), the volume of the lower and the upper phases, and the components of the upper phase gradually stabilize. DGA in the lower phase volume would reacts with CO_2 leading to a high viscosity.

3.4. Alcohol effect on regeneration energy of DGA-PMDETA

To investigate the impact of alcohol addition on biphasic absorbents, the energy consumption required for regenerating DGA-PMDETA biphasic absorbents is calculated. The specific heat capacity was characterized using DSC, as shown in Fig. S3. Energy consumption data, along with modifying factors for both 3D6P-1alcohol and 3D7P, were recorded and presented in Table 1.

The alcohol shows little impact on the regeneration energy of the DGA-PMDETA systems. The regeneration energy of 30 wt % MEA is 3.74 GJ/ton CO_2 (Zhu et al., 2019). The biphasic anhydrous absorbents reduce desorption energy consumption by 38 % on average compared to 30 wt % MEA. Theoretically, the energy consumption is related to the

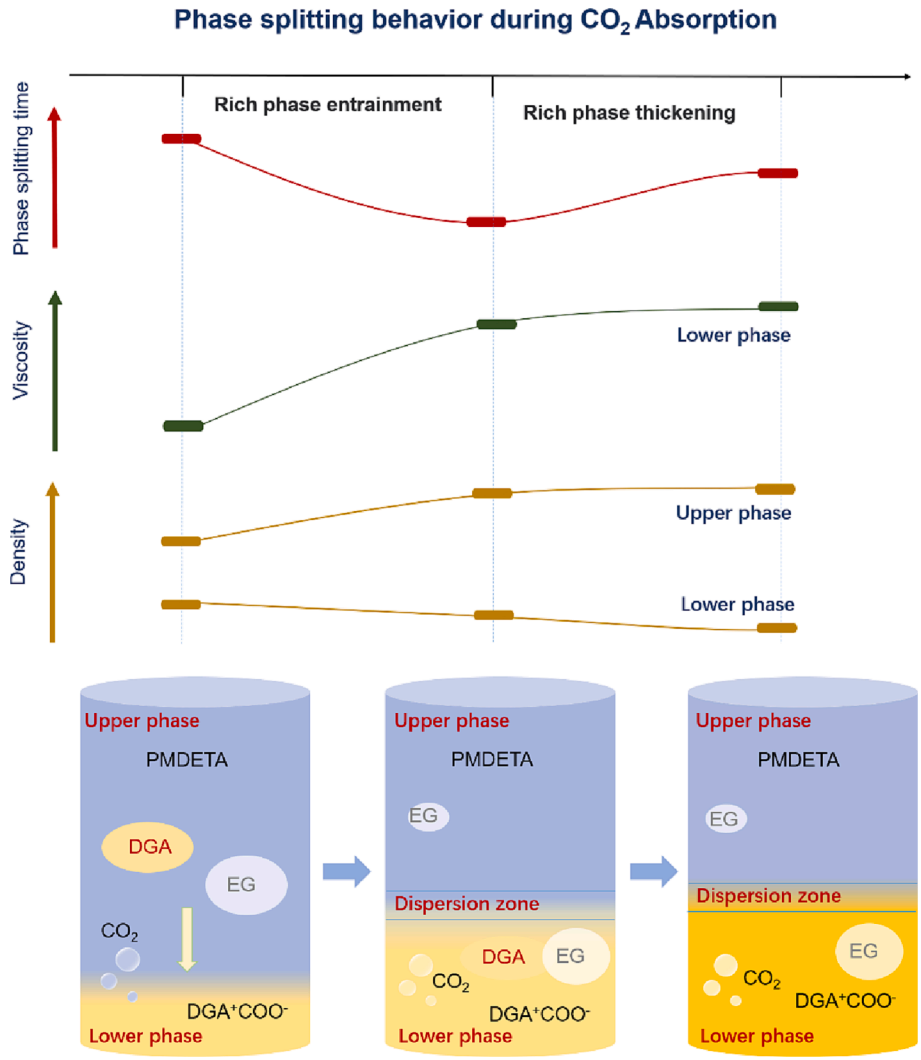

Fig. 6. The phase splitting behaviors of the DGA-PMDETA-alcohol system during CO_2 absorption.

Table 1
Regeneration energy of 3D6P-1alcohol and 3D7P (373 K).

	Cp (kJ·kg^{-1}·K^{-1})	χ	ΔT (K)	Ψ (%)	M (mpa·s)	Energy (GJ/ton CO_2)			
						Q_{reac}	Q_{sen}	Q^*_{sen}	Q^*_{reg}
3D7P	2.33	2.04	20	27	195	1.94	0.33	0.66	2.27
3D6P-1EG	2.45	1.62	20	36	63	1.94	0.40	0.65	2.26
3D6P-1BDO	2.25	1.83	20	36	95	1.94	0.37	0.68	2.28
3D6P-1PDO	2.52	2.06	20	36	96	1.94	0.41	0.85	2.37
3D6P-1Gl	2.30	2.44	20	36	161	1.94	0.38	0.92	2.40
3D6P-1NBA	2.33	2.02	20	27	192	1.94	0.33	0.66	2.27

viscosity and volume of the CO_2-rich phase, and specific heat capacity of various alcohols. The higher volume ratio of the rich phase in 3D6P-1 alcohol (2.26 to 2.40 GJ/ton CO_2) does not significantly impact energy consumption compared to that of 3D7P (2.27 GJ/ton CO_2). The viscosity shows a slightly greater influence on the energy consumption by affecting the correction factor χ. Although 3D6P-1EG and 3D6P-1PDO have comparable specific heat capacities and the same volume ratio of rich phase, their different viscosities result in a regeneration energy consumption that is 5 % higher for 3D6P-1PDO. Similarly, although 3D6P-1Gl and 3D6P-1NBA have comparable specific heat capacity and rich phase viscosity, their different volume ratios of rich phase lead to a regeneration energy that is 5 % higher for 3D6P-1Gl.

4. Conclusion

The CO_2 absorption, desorption, and phase splitting behaviors of anhydrous DGA-PMDETA systems were experimentally investigated to elucidate the impact of alcohols on a biphasic system consisting of primary/secondary amine and tertiary amine. The main findings of this study are summarized below:

1. At a mass ratio of DGA/PMDETA of 3:7, CO_2-rich phase shows a CO_2 loading of 3.67 mol CO_2/kg CO_2-rich phase, the volume ratio of 27 %, and viscosity of 3309 mPa·s. The addition of DBO, PDO, Gl, and EG as the dilutes are effective in reducing the viscosity of the CO_2-rich phase; while NBA transfers into the CO_2-lean phase. Specifically. The viscosity of 3D6P-1EG are lowered than others. The addition of alcohols does not affect the absorption loading or CO_2 absorption rate prior to phase separation.
2. Adding alcohols can regulate the viscosity of the rich phase, leading to a shorter phase splitting time. The process of phase splitting during CO_2 absorption could be divided into rich phase entrainment stage and rich phase thickening stage. As CO_2 loading increases, there is a gradual increase in both viscosity and density difference between the upper and lower phases. In the rich phase entrainment stage, DGA-CO_2 product collaborates with the majority of unreacted DGA and alcohols to transfer into the lower phase under gravity dominance, resulting in a reduction in phase splitting time as CO_2 loading increases. In the thickening stage of the rich phase, DGA in the lower phase reacts with CO_2, resulting in an increase in viscosity of the rich phase while maintaining a constant density difference between upper and lower phases. The time for phase splitting increases with CO_2 loading. Most DGA reacts with CO_2 in the lower phase after the beginning of phase splitting.
3. At a regeneration temperature of 353 K, the desorption rate of 3D6P-1EG was observed to be 19 % higher than that of 30 wt % MEA at 393 K, with a maximum achievable desorption rate of 89 %. The CO_2 product can be easily decomposed, resulting in a high regeneration rate. A correction factor for viscosity was introduced to calculate energy consumption during desorption of systems with high viscosity. Compared to 30 wt % MEA, the anhydrous biphasic absorbent demonstrated an average reduction of 38 % in regenerative energy consumption. Specifically, the regenerative energy consumption of 3D6P-1EG was measured as only 2.26 GJ/ton CO_2. Specific heat capacity, rich phase volume ratio, and rich phase viscosity were ranked in order of importance as influencing factors on desorption energy consumption. The higher the value of these factors, the greater the energy consumed during desorption.

Declaration of Competing Interest

The authors declare that they have no known competing financial interests or personal relationships that could have appeared to influence the work reported in this paper.

Data availability

No data was used for the research described in the article.

Acknowledgements

Thanks to the financial support from National Natural Science Foundation of China (21878190) and China Petrochemical Corporation (419033-1). Thanks to the Engineering Experimental Teaching Center, School of Chemical Engineering, Sichuan University for the Nuclear Magnetic Resonance (NMR, JNM-ECZ400S/L1, JEOL Ltd., Japan) support.

Appendix A. Supplementary data

Supplementary data to this article can be found online at https://doi.org/10.1016/j.ces.2023.119083.

References

Barnea, E., Mizrahi, J., 1975. Separation mechanism of liquid-liquid dispersions in a deep-layer gravity settler. part II - flow patterns of the dispersed and continuous phases within the dispersion band. Trans. Inst. Chem. Eng. 53, 70–74.
Barzagli, F., Mani, F., Peruzzini, M., 2017. Novel water-free biphasic absorbents for efficient CO_2 capture. Int. J. Greenh. Gas Control. 60, 100–109. https://doi.org/10.1016/j.ijggc.2017.03.010.
Deng, Q., Ling, X., Zhang, K., Tan, L., Qi, G., Zhang, J., 2022. CCS and CCUS technologies: giving the oil and gas industry a green future. Front, Energy Res https://doi.org/10.10.3389/fenrg.2022.919330.
Fang, M., Yi, N., Di, W., Wang, T., Wang, Q., 2020. Emission and control of flue gas pollutants in CO_2 chemical absorption system – a review. Int. J. Greenh. Gas Control. 93, 102904.
Jiang, C., Chen, H., Wang, J., Shen, Y., Ye, J., Zhang, S., Wang, L., Chen, J., 2020. Phase splitting agent regulated biphasic solvent for efficient CO_2 capture with a low heat duty. Environ Sci Technol. 54, 7601–7610. https://doi.org/10.1021/acs.est.9b07923.
Jiang, W., Wu, F., Gao, G., Li, X., Zhang, L., Luo, C., 2021. Absorption performance and reaction mechanism study on a novel anhydrous phase change absorbent for CO_2 capture. Chem. Eng. J. 420 https://doi.org/10.1016/j.cej.2021.129897.
Jin, X., Fang, J., Ma, Q., Wang, R., Zhang, W., 2022. Effect of amine properties on developing CO_2 phase change absorbents by means of cosolvent effect. Sep. Purif. Technol. 289 https://doi.org/10.1016/j.seppur. 2022.120630.
Kaul, A., Pereira, R.A.M., Asenjo, J.A., Merchuk, J.C., 1995. Kinetics of phase separation for polyethylene glycol-phosphate two-phase systems. Biotechnol. Bioeng. 48 (3), 246–256. https://doi.org/10.1002/bit.260480311.
Kim, Y.E., Park, J.H., Yun, S.H., Nam, S.C., Jeong, S.K., Yoon, Y.I., 2014. Carbon dioxide absorption using a phase transitional alkanolamine–alcohol mixture. J. Ind. Eng. Chem. 20, 1486–1492. https://doi.org/10.1016/j. jiec.2013.07.036.
Kortunov, P.V., Baugh, L.S., Siskin, M., Calabro, D.C., 2015. In situ nuclear magnetic resonance mechanistic studies of carbon dioxide reactions with liquid amines in

mixed base systems: the interplay of lewis and brønsted basicities. Energy Fuels. 29, 5967–5989. https://doi.org/10.1021/acs.energyfuels.5b00988.
Kortunov, P.V., Siskin, M., Paccagnini, M., Thomann, H., 2016. CO2 reaction mechanisms with hindered alkanolamines: control and promotion of reaction pathways. Energy Fuels. 30, 1223–1236. https://doi.org/10.1021/acs.energyfuels.5b02582.
Li, L., Rochelle, G., 2014. CO2 mass transfer and solubility in aqueous primary and secondary amine. Energy Procedia 63, 1487–1496. https://doi.org/10.1016/j.egypro.2014.11.158.
Li, X., Wang, S., Chen, C., 2013. Experimental study of energy requirement of CO_2 desorption from rich solvent. Energy Procedia. 37, 1836–1843. https://doi.org/10.1016/j.egypro.2013.06.063.
Li, X., Wang, Y., Lu, H., Zhong, S., Liu, C., Song, L., Tang, S., Liang, B., 2022. Phase splitting rules of the primary/secondary amine-tertiary amine systems: experimental rapid screening and corrected quasi-activity coefficient model. Ind. Eng. Chem. Res. 61, 7709–7717. https://doi.org/10.1021/acs.iecr.2c00533.
Li, J., You, C., Chen, L., Ye, Y., Qi, Z., Sundmacher, K., 2012. Dynamics of CO_2 absorption and desorption processes in alkanolamine with cosolvent polyethylene glycol. Ind. Eng. Chem. Res. 51, 12081–12088. https://doi.org/10.1021/ie301164v.
Lin, J., Huang, K., Suo, Z., Li, X., Xiao, C., Liu, H., 2015. Phase separation dynamics in oil-polyethylene glycol–sulfate–water based three-liquid-phase systems. Ind. Eng. Chem. Res. 54, 3952–3960. https://doi.org/10.1021/acs.iecr.5b00066.
Liu, F., Fang, M., Dong, W., Wang, T., Xia, Z., Wang, Q., Luo, Z., 2019a. Carbon dioxide absorption in aqueous alkanolamine blends for biphasic solvents screening and evaluation. Appl. Energy. 233–234, 468–477. https://doi.org/10.1016/j.apenergy.2018.10.007.
Liu, F., Fang, M., Yi, N., Wang, T., Wang, Q., 2019b. Biphasic behaviors and regeneration energy of a 2-(diethylamino)-ethanol and 2-((2-aminoethyl)amino) ethanol blend for CO_2 capture. Sustain. Energy Fuels. 3, 3594–3602. https://doi.org/10.1039/c9se00821g.
Mlllard, M., 2020. Lange's handbook of chemistry [M]. J. Assoc. Off. Anal. Chem. 6, 6.
Mores, P., Scenna, N., Mussati, S., 2011. Post-combustion CO_2 capture process: Equilibrium stage mathematical model of the chemical absorption of CO_2 into monoethanolamine (MEA) aqueous solution. Chem Eng Res Des. 89, 1587–1599. https://doi.org/10.1016/j.cherd.2010.10.012.
Nawaz, M., Suleman, H., Maulud, A.S., 2022. Carbon capture and utilization: a bibliometric analysis from 2007–2021. Energies. 15, 6611. https://doi.org/10.3390/en15186611.
Nwaoha, C., Idem, R., Supap, T., Saiwan, C., Tontiwachwuthikul, P., Rongwong, W., Al-Marri, M.J., Benamor, A., 2017. Heat duty, heat of absorption, sensible heat and heat of vaporization of 2–Amino–2–Methyl–1–propanol (AMP), piperazine (PZ) and monoethanolamine (MEA) tri–solvent blend for carbon dioxide (CO_2) capture. Chem. Eng. Sci. 170, 26–35. https://doi.org/10.1016/j.ces.2017.03.025.
Papadopoulos, A.I., Tzirakis, F., Tsivintzelis, I., Seferlis, P., 2019. Phase-change solvents and processes for postcombustion CO_2 capture: a detailed review. Ind. Eng. Chem. Res. 58, 5088–5111. https://doi.org/10.1021/acs.iecr.8b06279.
Pinto, D.D.D., Zaidy, S.A.H., Hartono, A., Svendsen, H.F., 2014. Evaluation of a phase change solvent for CO_2 capture: Absorption and desorption tests. Int. J. Greenh. Gas Control. 28, 318–327. https://doi.org/10.1016/j.ijggc.2014.07.002.
Salkuyeh, Y.K., Mofarahi, M., 2012. Comparison of MEA and DGA performance for CO_2 capture under different operational conditions. Int. J. Energy Res. 36, 259–268. https://doi.org/10.1002/er.1812.
Santos, I.J., Carvalho, R.M., Silva, M.A., Silva, L.H., 2012. Phase diagram, densities, and the refractive index of new aqueous two-phase system formed by PEO1500 + thiosulfate + H_2O at different temperatures. J. Chem. Eng. Data. 57, 274–279. https://doi.org/10.1021/je200744s.
Sarmad, S., Mikkola, J.P., Ji, X., 2017. Carbon dioxide capture with ionic liquids and deep eutectic solvents: a new generation of sorbents. Chem. Sus. Chem. 10, 324–352. https://doi.org/10.1002/cssc.201600987.
Shakerian, F., Kim, K.-H., Szulejko, J.E., Park, J.-W., 2015. A comparative review between amines and ammonia as sorptive media for post-combustion CO_2 capture. Appl. Energy. 148, 10–22. https://doi.org/10.1016/j.apenergy.2015.03.026.
Shen, Z., Chang, D., Guo, B., Lu, H., Ji, Y., Tang, S., Mao, S., Liang, B., 2023. Effect of water on CO_2 capture performance of anhydrous phase change absorbent. Low-carbon Chem. and Chem, Eng https://kns.cnki.net/kcms2/article/abstract?urlId=51.1807.TQ.20230607.1437.004&uniplatform=NZKPT.
Wang, N., Peng, Z., Gao, H., Sema, T., Shi, J., Liang, Z., 2022. New insight and evaluation of secondary Amine/N-butanol biphasic solutions for CO_2 Capture: Equilibrium Solubility, phase separation Behavior, absorption Rate, desorption Rate, energy consumption and ion species. Chem. Eng. J. 431, 133912.
Xu, M., Wang, S., Xu, L., 2019. Screening of physical-chemical biphasic solvents for CO_2 absorption. Int. J. Greenh. Gas Control. 85, 199–205. https://doi.org/10.1016/j.ijggc.2019.03.015.
Zhan, X., Lv, B., Yang, K., Jing, G., Zhou, Z., 2020. Dual-functionalized ionic liquid biphasic solvent for carbon dioxide capture: high-efficiency and energy saving. Environ. Sci. Technol. 54, 6281–6288. https://doi.org/10.1021/acs.est.0c00335.
Zhang, S., Shen, Y., Shao, P., Chen, J., Wang, L., 2018. Kinetics, Thermodynamics, and Mechanism of a Novel Biphasic Solvent for CO_2 Capture from Flue Gas. Environ. Sci. Technol. 52, 3660–3668. https://doi.org/10.1021/acs.est.7b05936.
Zhang, S., Shen, Y., Wang, L., Chen, J., Lu, Y., 2019. Phase change solvents for post-combustion CO_2 capture: Principle, advances, and challenges. Appl. Energy. 239, 876–897. https://doi.org/10.1016/j.apenergy.2019.01.242.
Zhao, X., 2021. Quantitative structure-property relationship study on carbon dioxide absorption with phase-splitting system of amine-organic solvent-water. Sichuan University, Sichuan.
Zhao, H., Li, X., Wu, X., 2018. New friction factor and Nusselt number equations for turbulent convection of liquids with variable properties in circular tubes. Int. J. Heat Mass Transf. 124, 454–462. https://doi.org/10.1016/j.ijheatmasstransfer.2018.03.082.
Zhao, X., Li, X., Liu, C., Zhong, S., Lu, H., Yue, H., Ma, K., Song, L., Tang, S., Liang, B., 2022. The quasi-activity coefficients of non-electrolytes in aqueous solution with organic ions and its application on the phase splitting behaviors prediction for CO_2 absorption. Chin. J. Chem. Eng. 43, 316–323. https://doi.org/10.1016/j.cjche.2022.02.003.
Zhou, X., Liu, F., Lv, B., Zhou, Z., Jing, G., 2017. Evaluation of the novel biphasic solvents for CO2 capture: Performance and mechanism. Int. J. Greenh. Gas Control. 60, 120–128. https://doi.org/10.1016/j.ijggc.2017.03.013.
Zhou, X., Li, X., Wei, J., Fan, Y., Liao, L., Wang, H., 2020. Novel nonaqueous liquid-liquid biphasic solvent for energy-efficient carbon dioxide capture with low corrosivity. Environ. Sci. Technol. 54, 16138–16146. https://doi.org/10.1021/acs.est.0c05774.
Zhu, K., Lu, H., Liu, C., Wu, K., Jiang, W., Cheng, J., Tang, S., Yue, H., Liu, Y., Liang, B., 2019. Investigation on the phase-change absorbent system MEA + solvent A (SA) + H_2O used for the CO_2 capture from flue gas. Ind. Eng. Chem. Res. 58, 3811–3821. https://doi.org/10.1021/acs.iecr.8b04985.
Zhu, X., Lu, H., Wu, K., Zhu, Y., Liu, Y., Liu, C., Liang, B., 2020. DBU-glycerol solution: a CO_2 absorbent with high desorption ratio and low regeneration energy. Environ. Sci. Technol. 54, 7570–7578. https://doi.org/10.1021/acs.est.0c01332.